Journal of
Materials Chemistry A

Materials for energy and sustainability

Accepted Manuscript

This article can be cited before page numbers have been issued, to do this please use: M. S. Abbasi, C. Li, J. Gao, S. Wang, S. Wang, Q. Lin, X. Gening, S. N. Khan, J. Zhang, X. Zhang, Y. Cai and H. Huang, *J. Mater. Chem. A*, 2024, DOI: 10.1039/D4TA06013J.

ROYAL SOCIETY OF CHEMISTRY

rsc.li/materials-a

View Article Online
DOI: 10.1039/D4TA06013J

High Performance All-Polymer Solar Cells Enabled with Solvent and Solid Dual Additives

Received 00th January 20xx,
Accepted 00th January 20xx

DOI: 10.1039/x0xx00000x

Misbah Sehar Abbasi,[a] Congqi Li,[a] Jinhua Gao,[a] Siying Wang,[a] Sixuan Wang,[a] Qijie Lin,[a] Xie Gening,[a] Saqib Nawaz Khan,[b] Jianqi Zhang,[c] Xin Zhang,[a] Yunhao Cai*[a] and Hui Huang*[a]

Morphology optimization of photoactive layer plays a crucial role in fabricating high-performance polymer solar cells (PSCs). When an active layer is cast from solution, the unique properties of the donor and acceptor materials often lead to either excessive or insufficient phase separation, which adversely affect the performance of the device. Specifically, all-polymer solar cells (all-PSCs) introduce an added complexity in terms of morphology regulation due to the inherently flexible and entangled nature of polymer chains. In this work, we first introduced 3,5-dichloroanisole (DCA) as a solid additive, known for its good crystallinity and volatility, to refine the active layer morphology in all-PSCs. Then, we combined 1-chloronaphthalene (CN) and DCA as dual additives, which effectively optimized the morphology of all-polymer blend. This combination favors charge transport and minimizes charge recombination, leading to higher fill factor across various systems. Notably, device based on PM6:PY-DT processed with this dual-additives approach achieved an impressive power conversion efficiency (PCE) of 17.42%, outperforming the control device without any additive, which showed a PCE of 14.34%. Besides, the dual additives were applied in the other systems, revealing its universality. This work not only took advantages of both solvent and solid additives, but also effectively improved the performance of all-PSCs.

1 Introduction

Polymer solar cells (PSCs) have emerged as a promising energy-harvesting technology for green energy, thanks to their solution processability, lightweight, and flexibility.[1–6] The efficiency of small molecule-based PSCs has significantly increased recently owing to the swift progress in small-molecule acceptors (SMAs), illustrating their great potential of commercialization.[7–21] Generally, all-PSCs are considered more suitable for the practical use due to their excellent stretchability, mechanical robustness, and photo-thermal stability.[22–28] However, all-PSCs have received less attention and their power conversion efficiencies (PCEs) are comparatively lower than SMA-based counterparts.[29–36] One fundamental reason for their inferior performance lies in the difficulty in morphological control.[37–39] The unique characteristics of the polymer donor and acceptor materials, as well as the big molecular size of the polymers increase the difficulty in morphology control.[40,41] In addition, the slow diffusion of polymer components during active-layer formation further lead to inadequate or excessive phase separation.[42] Consequently, effective morphological control methods are substantially needed to adjust the phase separation for improving the performance of all-PSCs.

Much efforts have been devoted to optimize the morphology of the PSC, such as solvent vapor annealing, thermal annealing, solvent additive treatment and hot solution casting etc. Among them, solvent additive is a widely adopted strategy of facially tuning the film morphology.[43–48] The morphology of PSCs can be well-manipulated by adding a tiny amount of the proper additive into the host system.[49–52] The influence of solvent additives on morphological control is associated with two characteristics: limited solvency to either donor or acceptor and low volatility.[53] This indicates that solvent additives have less volatile nature (due to high boiling point) than host solvent, which can effectively manipulate aggregation of both donor and acceptor and hence form desired phase separation during film formation. Besides solvent additives, solid additives with high crystallinity have attracted intense interests, since they also show a favorable effect on controlling the self-assembly and phase separation of photovoltaic materials via various intermolecular interactions.[43,53–58] It has been proved that both solvent and solid additives can improve the performance of solar cell. Therefore, the combination of two kinds of additive is considered as a simple yet effective approach to optimizing the morphology of active layer. Nevertheless, morphological optimization involving two additives simultaneously and its impact on the photovoltaic performance of PSCs has been seldom investigated.[53,57,59–61]

Here, we developed a new strategy of tuning the morphology of all-polymer systems via incorporating the synergistic effects of solvent additive and volatilizable solid additive to achieve high performance PSCs. Upon the use of the dual additives (CN+DCA), PM6:PY-DT based all-PSC realized a PCE of 17.42%, outperforming the devices processed with CN (16.42%) or DCA (16.57%). Systematic characterizations revealed that the enhanced efficiency is attributed to the optimized morphology, facilitated charge transport and suppressed charge recombination. In addition, the developed dual additives (CN+DCA) were also successfully applied into PM6:PY-IT and PM6:PYF-T-o based PSCs, demonstrating the universality of the strategy.

[a] College of Materials Science and Opto-Electronic Technology Center of Materials Science and Optoelectronics Engineering CAS Center for Excellence in Topological Quantum Computation CAS Key Laboratory of Vacuum Physics, University of Chinese Academy of Sciences, Beijing 100049, China.
[b] Institute of Physics, Chinese Academy of Sciences, Beijing 100190, China
[c] CAS Key Laboratory of Nanosystem and Hierarchical Fabrication, CAS Center for Excellence in Nanoscience, National Center for Nanoscience and Technology, Beijing 100190, China. Email: caiyunhao@ucas.ac.cn; huihuang@ucas.ac.cn

View Article Online
DOI: 10.1039/D4TA06017J

2 Results and Discussions

Fig. 1a exbibits molecular structures of PM6, PY-DT, CN and DCA. CN and DCA were selected as solvent and solid additive, respectively. The energy levels of PM6 and PY-DT were estimated by cyclic voltammetry measurement (Fig. 1c). The normalized UV-vis absorption spectra of pristine films of PM6, PY-DT, DCA and the blend films are shown in Fig. 1d,1e and Fig. S1, respectively. It was found that upon the use of dual additives, the absorption coefficient was obviously increased, which may benefit the J_{sc} of corresponding device. To study the volatility of solid additive DCA, thermogravimetry analysis (TGA) was carried out at first, which demonstrates that DCA underwent a gradual and continuous weight loss starting from 33 ℃ and reaching zero at ~90℃ (shown in Fig. S2), suggesting the material was totally volatilized. This result indicates that DCA can be completely removed from the blend films after thermal annealing (TA) procedure.

To study the effect of CN+DCA dual additives on photovoltaic performance of PSCs, a series of devices with a conventional architecture of ITO/PEDOT:PSS/active layer/PNDIT:F3N/Ag were fabricated (Fig. 1b). Fig. 2a illustrates the current density-voltage (*J-V*) curves of optimized PM6:PY-DT based PSCs under standard AM 1.5G illumination with 100 mW cm^{-2}. The photovoltaic parameters including V_{oc}, J_{sc}, FF and PCE are summarized in Table 1 and Table S1. PM6:PY-DT based devices without any additive (Device-I) achieved a PCE of 14.34% with a V_{oc} of 0.970 V, a J_{sc} of 23.86 mA cm^{-2} and an FF of 62.03%. While the PM6:PY-DT device processed with a solvent additive of CN (Device-II) showed a PCE of 16.42% with a V_{oc} of 0.962 V, a J_{sc} of 23.96 mA cm^{-2} and an FF of 71.20%. PM6:PY-DT based devices with DCA as a solid additive (Device-III) afforded a higher PCE of 16.57% with a V_{oc} of 0.974 V, a J_{sc} of 24.48 mA cm^{-2} and an FF of 69.44%. Impressively, PM6:PY-DT based devices with the dual additives (Device-IV) has secured an enhanced PCE of 17.42% with V_{oc}, J_{sc} and FF reaching up to 0.977 V, 24.57 mA cm^{-2} and 72.60%, respectively. The J_{sc} values were further validated by the external quantum efficiency (EQE) measurement as demonstrated in Fig. 2b. Overall, all of the devices showed high and broad EQE response in the wavelength range of 300-900 nm. Specifically, Device I-IV exhibited integrated current densities (J_{cal}) of 23.06, 23.18, 23.58 and 23.71 mA cm^{-2},

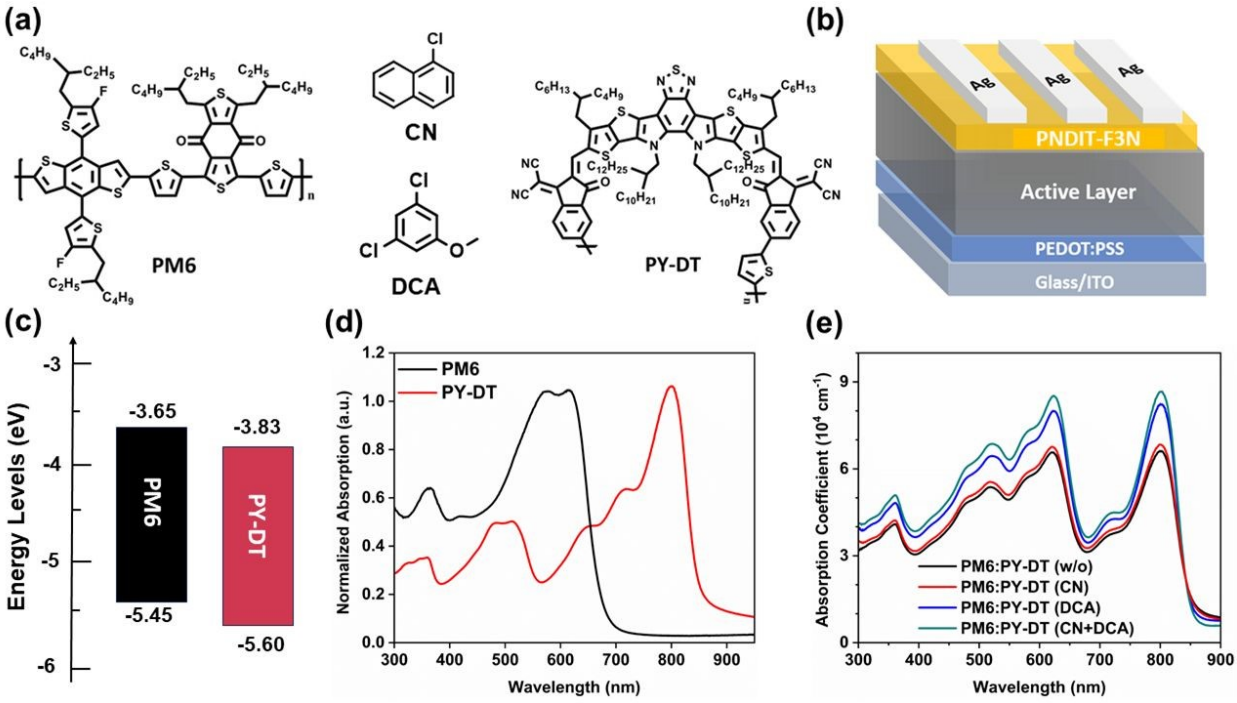

Fig. 1 (a) Chemical structures of PM6, PY-DT, CN and DCA. (b) Conventional device structure of PSCs. (c) Energy levels of PM6 and PY-DT. (d) Normalized absorption spectra of pristine films. (e) UV-vis absorption spectra of PM6:PY-DT blend films with different additive treatments.

Table 1 Photovoltaic parameters of PM6:PY-DT based devices fabricated with different additives

Additive	V_{oc} (V)	J_{sc} (mA cm^{-2})	FF (%)	PCE[a] (%)
w/o	0.970 (0.970±0.02)	23.86 (23.85±0.10)	62.03 (61.90±0.55)	14.34 (14.31±0.27)
CN	0.962 (0.968±0.05)	23.96 (23.90±0.12)	71.20 (71.15±0.72)	16.42 (16.34± 0.25)
DCA	0.974 (0.970±0.04)	24.48 (24.42±0.25)	69.44 (69.10±0.63)	16.57 (16.35±0.29)
CN + DCA	0.977 (0.974±0.003)	24.57 (24.50±0.15)	72.60 (71.87±0.30)	17.42 (17.36±0.10)

[a] The numerical values in brackets were obtained from statistical data of 10 independent devices.

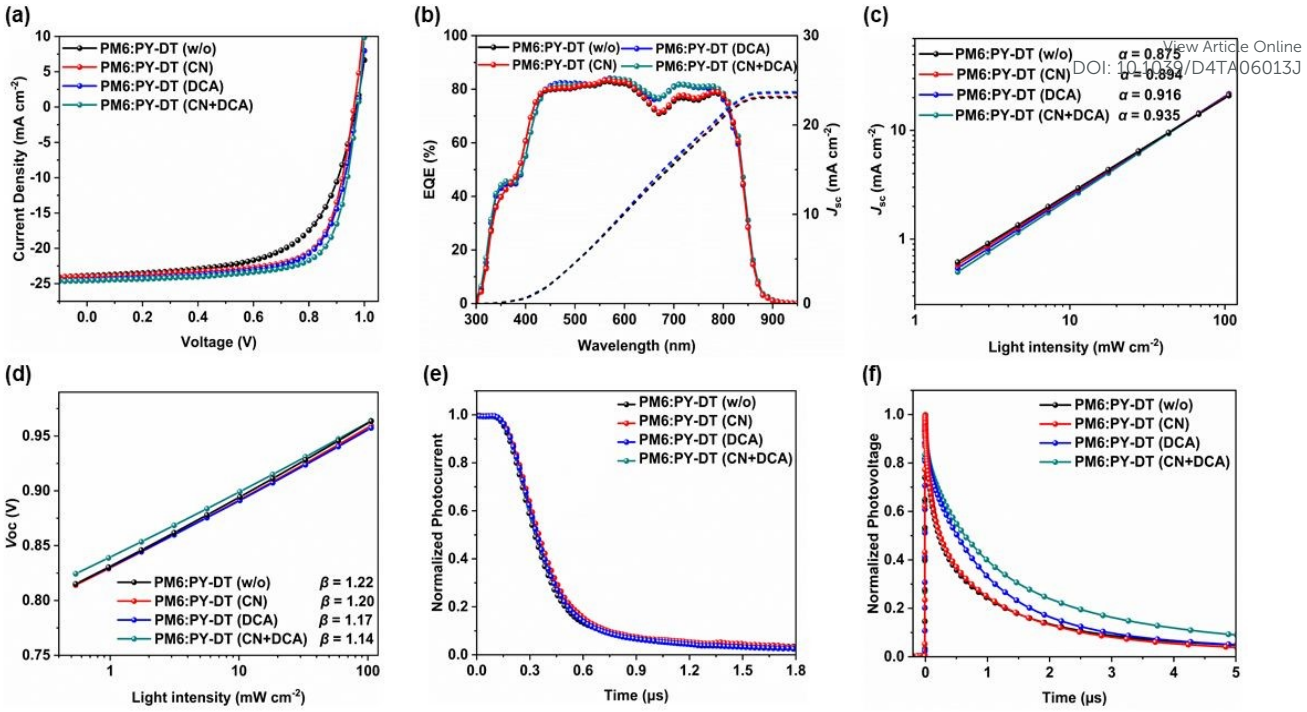

Fig. 2 (a) *J-V* characteristics and, (b) EQE spectra and integrated J_{sc} of PM6:PY-DT fabricated under various conditions. (c) J_{sc} vs light intensity and, (d) V_{oc} vs light intensity. (e) TPC and, (f) TPV of PM6:PY-DT fabricated under various conditions.

respectively, which are in good agreement with the values obtained from *J-V* measurements.

To study influence of dual additives on the kinetics of charge recombination in PM6:PY-DT based devices, both the J_{sc} and V_{oc} were plotted with respect to light intensity (P_{light}) as shown in Fig. 2c and Fig. 2d respectively. The relationship between P_{light} and J_{sc} can be expressed as $J_{sc} \propto P_{light}^{\alpha}$, in which α is the slope of the curve. If the α is close to 1, the bimolecular recombination is suppressed under the short-circuit condition. The α values for the Device I-III were determined to be 0.875, 0.894, 0.916, respectively, while that of Device IV exhibited a higher value of 0.935, which suggests that a reduced bimolecular recombination in the Device IV, and thus contributed to the higher FF. The charge recombination kinetics of the devices were then explored by measuring the dependence of V_{oc} on the P_{light}. If the slope of V_{oc} versus the natural logarithm of P_{light} equals to $\beta kT/q$, bimolecular recombination plays a major role inside the device, where k is the Boltzmann constant, T is the Kelvin temperature and q is the elementary charge. When trap-assisted recombination is involved, a strong dependency of V_{oc} on the light intensity ($>kT/q$) will be obtained. The β vlaues for Device I-IV are 1.22, 1.20, 1.17, and 1.14, respectively, which shows that the trap assisted recombination has been suppressed by the dual additives.

The effect of dual additives on carrier lifespan and charge extraction time of the PM6:PY-DT devices were evaluated by transient photovoltage (TPV) and transient photocurrent (TPC) measurements. Fig. 2e presented the TPC curves of PM6: PY-DT devices with different additives treatment under various light intensities. The charge extraction time derived by fitting the TPC curves for Device I-III were 0.31, 0.22, and 0.20 μs, respectively, larger than that of Device-IV (0.18 μs). Therefore, it can be inferred that the dual additives favor charge extraction in comparison to the other systems. The TPV curves of Device I-IV under various light intensities are exhibited in Fig. 2f. The carrier lifetime of Device I-III was determined to be 0.66, 0.72, and 1.02 μs, respectively, shorter than that of Device-IV (1.25 μs). This observation suggested that dual-additives can be effective in increasing the charge mobility and reducing the charge recombination.

To investigate the effect of dual additive on charge generation and dissociation processes, a graph between photocurrent density (J_{ph}) and effective voltage (V_{eff}) was plotted (Fig. S3). J_{ph} is defined as $J_{ph} = J_L - J_D$, and V_{eff} is denoted as $V_{eff} = V_0 - V_a$, in which V_0 is the voltage at which J_{ph} is zero, and V_a is the applied bias voltage. When the J_{ph} reaches saturation at V_{eff} of 2V, the saturation values (J_{sat}) of Device I-IV were 25.17, 24.94, 25.21, and 25.26 mA cm^{-2}, respectively. The exciton dissociation probability $P(E,T)$ was accessed by normalizing J_{ph} with respect to J_{sat} (J_{ph}/J_{sat}) under the short-circuit conditions. The $P(E,T)$ values of Device I-IV were 94.7%, 96%, 97% and 97.2%, respectively. These observations revealed that the dual-additives is beneficial for charge generation and dissociation processes. The space-charge limited current (SCLC) method was carried out to explore the charge mobilities of Device I-IV. Devices with configurations of ITO/PEDOT:PSS/active layer/MoO_3/Ag and ITO/ZnO/active layer/PNDIT-F3N/Ag were fabricated to obtain the hole and electron mobilities, respectively. Fig. S4 illustrates the plots of $J^{1/2}$ -*V* for electron-only and hole-only devices, and Table S2 summarizes the corresponding electron (μ_e) and hole (μ_h) mobilities. Among Device I- IV, Device IV processed with dual additives exhibited

the highest μ_e and μ_h of 3.40×10^{-4} and 3.19×10^{-4} cm^2 V^{-1} s^{-1}, respectively. Besides, the ratios of the hole/electron mobility μ_h/μ_e are 1.50, 1.29,1.25, and 1.06 for Device I-IV, respectively. The highest mobility and most balanced charge transport properties of Device IV processed with dual additives may contribute to the highest J_{sc} and FF.

To investigate the miscibility of DCA between PM6 and PY-DT by Flory-Huggins interaction parameter (χ), contact angle measurements were performed as illustrated in Fig. S5. The surface free energy (γ) of PM6, PY-DT and DCA calculated by Wu's model were 25.76, 26.60 and 28.96 mN m^{-1}, respectively (Table S3). The Flory-Huggins interaction parameters of PM6/DCA, PY-DT/PM6, and PY-DT/DCA were calculated to be 1.79, 1.1 and 0.16 respectively, which suggests that DCA has higher miscibility with PY-DT in contrast to PM6. Due to the favorable miscibility of DCA and PY-DT, DCA can restrain the over self-assembly of PY-DT amidst the film-casting process, leading to a conducive PM6 and PY-DT matrix after DCA elimination during the TA treatment.

Atomic force microscopy (AFM) technique was employed to examine the surface morphology of PM6:PY-DT blend films subjected to various processing conditions as shown in Fig. 3 (a-d) and Fig. S6 (a-d). Obviously, the PM6:PY-DT blend film of Device I exhibited smooth surface with large crystalline bulk and root mean square (RMS) of 1.00 nm. The blend processed with CN revealed RMS of 0.90 nm, while the blend using DCA as solid additive presented a RMS of 1.15 nm. Particularly, dual additives treated blend (Device IV) showed improved crystallization which helps in polymer growth with a RMS of 1.49 nm. Figure S7 exhibits the TEM images of the blends, it can be observed that the blend film treated by dual additives showed a more obvious fibrillar morphology. This is beneficial to efficient exciton dissociation and charge transport.

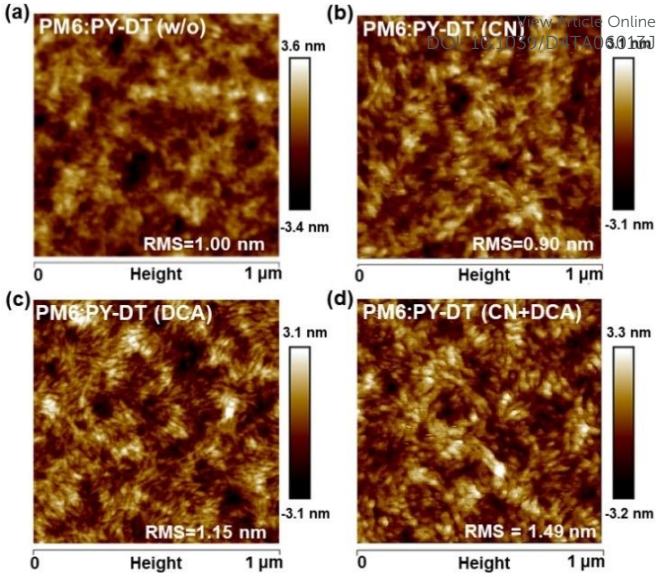

Fig. 3 (a-d) AFM height images of the PM6:PY-DT blend films fabricated under various conditions.

To examine the molecular packing and crystallinities of PM6:PY-DT blend films, grazing-incidence wide angle X-ray scattering (GIWAXS) analyses were conducted. Fig. 4 displays both the two-dimensional (2D) GIWAXS patterns and their respective line cuts, and the comprehensive summary of diffraction peaks are provided in Table S4 and Table S5, respectively. PM6:PY-DT (w/o) film exhibited clear π–π stacking (010) peaks at q_z=1.650 (d-spacing=3.80 Å) along out-of-plane (OOP) direction and lamellar stacking (100) peaks at q_{xy}=0.304 (d-spacing=20.65 Å) along in-plane (IP) direction, suggesting that the molecular packing is preferably face-on oriented with regard to substrate. Upon adding CN or DCA additives in PM6:PY-DT blends, CCL

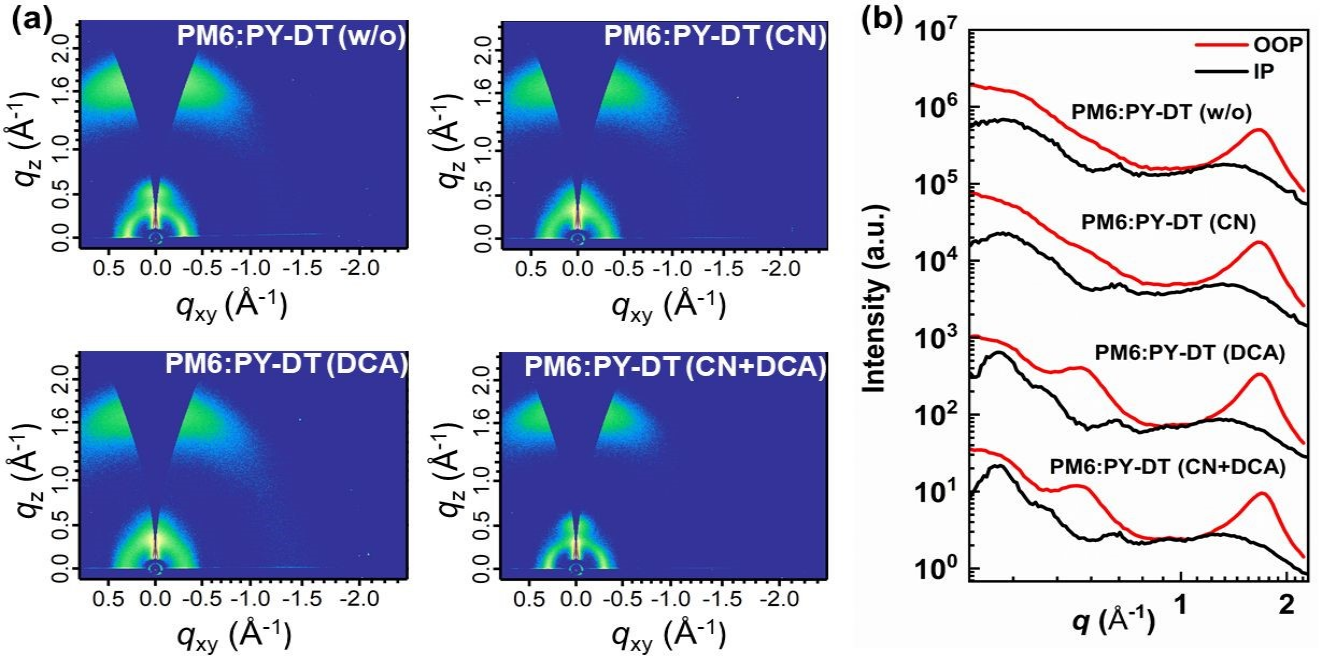

Fig. 4 (a) 2D GIWAXS scattering patterns of PM6:PY-DT blends fabricated under various conditions. (b) Line-cut profiles in IP and OOP directions from GIWAXS images of PM6:PY-DT blends fabricated under various conditions

values related to both the lamellar (100) and π–π stacking (010) peaks have increased, which suggests that CN and DCA can both improve the crystallinity and molecular order of PM6:PY-DT blend. The PM6:PY-DT blend films with the dual additive treatment exhibited a stronger π-π stacking (010) peak and a higher CCL from 17.00 to 22.15 Å. Furthermore, similar trend was observed along lamellar stacking where CCL values were increased from 102.16 to 107.27 Å. This translates that the blend film with dual additives has a more ordered crystalline structure. With the synergistic effect of CN and DCA, the molecular packing was effectually adjusted, which is advantageous for achieving higher charge carrier mobility and FF in the corresponding devices.

To investigate the generality of the dual additives, we further applied the strategy into PM6:PY-IT and PM6:PYF-T-o systems (Fig. S8). Figure S9a and S10a shows the *J-V* curves of the corresponding devices with different treatments. Table S6 and S7 summarizes the photovoltaic parameters of the corresponding devices. PM6:PY-IT without any additive achieved a PCE of 15.27%. Impressively, PM6:PY-IT based devices with the dual additives of CN+DCA has secured a remarkable PCE of 16.76%. The PM6:PYF-T-o based PSCs processed without additive showed a PCE of 12.24%. As expected, dual additives' treatment markedly increased the PCE to 16.37%. The improved J_{sc} has been further confirmed by the EQE test. It is worth mentioning that the synergistic effect of the CN and DCA resulted in significantly enhanced FF values and higher PCEs of the corresponding PSCs.

To address the stability requirements for practical applications, we further investigated the storage stability of unencapsulated devices. PM6:PY-DT based devices processed under different conditions have been stored in N_2 filled glove box. The T_{80} (the time required to reach 80% of initial performance) of all-PSCs processed with CN, DCA and CN+DCA is 473, 794 and 670 h, respectively as shown in Figure S11. This highlights the importance of additive selection for enhancing the long-term stability of all-polymer solar cells. These findings convincingly demonstrate that the introduction of dual additives synergistically enhances both device performance and stability.

3 Conclusion

In conclusion, we have able to develop a novel dual additives strategy to regulate the morphology of all-polymer blend, in which a solid additive DCA were combined with CN to synergistically optimize the molecular organization and phase separation. These improvements aid in enhancing charge transport and extraction efficiency while reducing charge recombination. Consequently, the PM6:PY-DT based OSCs treated with dual additives achieved a PCE of 17.42%, much higher than that of the devices without any additive (14.34%). Moreover, this approach has been successfully extended to other material systems, manifesting its universality. This work provides a new idea of regulating bulk heterojunction morphology towards the development of highly efficient all-PSCs.

Conflict of Interest

View Article Online
DOI: 10.1039/D4TA06013J

The authors declare no conflict of interest.

Data availability

The data that support the findings of this study are available in ESI.

Acknowledgements

The authors acknowledge the financial support from the NSFC (52103352, 51925306, and 52120105006), National Key R&D Program of China (2018FYA0305800), Key Research Program of Chinese Academy of Sciences (XDPB08-2), the Strategic Priority Research Program of Chinese Academy of Sciences (XDB28000000), the Youth Innovation Promotion Association of Chinese Academy of Sciences (2022165), and the Fundamental Research Funds for the Central Universities. Author was sponsored by ANSO scholarship for young talent.

References

1 G. Yu, J. Gao, J. C. Hummelen, F. Wudl and A. J. Heeger, *Science (80-.).*, 1995, **270**, 1789–1791.
2 A. Khasbaatar, Z. Xu, J.-H. Lee, G. Campillo-Alvarado, C. Hwang, B. N. Onusaitis and Y. Diao, *Chem. Rev.*, 2023, **123**, 8395–8487.
3 B. Liu, R.-Q. Png, L.-H. Zhao, L.-L. Chua, R. H. Friend and P. K. H. Ho, *Nat. Commun.*, 2012, **3**, 1321.
4 K. Weng, L. Ye, L. Zhu, J. Xu, J. Zhou, X. Feng, G. Lu, S. Tan, F. Liu and Y. Sun, *Nat. Commun.*, 2020, **11**, 2855.
5 D. Baran, R. S. Ashraf, D. A. Hanifi, M. Abdelsamie, N. Gasparini, J. A. Röhr, S. Holliday, A. Wadsworth, S. Lockett, M. Neophytou, C. J. M. Emmott, J. Nelson, C. J. Brabec, A. Amassian, A. Salleo, T. Kirchartz, J. R. Durrant and I. McCulloch, *Nat. Mater.*, 2017, **16**, 363–369.
6 H. Kang, G. Kim, J. Kim, S. Kwon, H. Kim and K. Lee, *Adv. Mater.*, 2016, **28**, 7821–7861.
7 H. Li, B. Yu and H. Yu, *Adv. Funct. Mater.*, 2024, **34,** 2402128.
8 S. Shen, Y. Mi, Y. Ouyang, Y. Lin, J. Deng, W. Zhang, J. Zhang, Z. Ma, C. Zhang, J. Song and Z. Bo, *Angew. Chemie Int. Ed.*, 2023, **62,** e202316495.
9 J. Fu, Q. Yang, P. Huang, S. Chung, K. Cho, Z. Kan, H. Liu, X. Lu, Y. Lang, H. Lai, F. He, P. W. K. Fong, S. Lu, Y. Yang, Z. Xiao and G. Li, *Nat. Commun.*, 2024, **15**, 1830.
10 L. Tian, C. Liu and F. Huang, *Sci. China Chem.*, 2024, **67**, 788–805.
11 Z. Li, K. Jiang, G. Yang, J. Y. L. Lai, T. Ma, J. Zhao, W. Ma and H. Yan, *Nat. Commun.*, 2016, **7**, 13094.
12 Y. Wei, Z. Chen, G. Lu, N. Yu, C. Li, J. Gao, X. Gu, X. Hao, G. Lu, Z. Tang, J. Zhang, Z. Wei, X. Zhang and H. Huang, *Adv. Mater.*, 2022, **34,** 2204718.
13 J. Gao, N. Yu, Z. Chen, Y. Wei, C. Li, T. Liu, X. Gu, J. Zhang, Z. Wei, Z. Tang, X. Hao, F. Zhang, X. Zhang and H. Huang, *Adv. Sci.*, 2022, **9,** 2203606.
14 H. Chen, W. Sun, R. Zhang, Y. Huang, B. Zhang, G. Zeng, J.

View Article Online
DOI: 10.1039/D4TA06013J

Ding, W. Chen, F. Gao, Y. Li and Y. Li, *Adv. Mater.*, 2024, **36,** 2402350.

15 X. Xu, W. Jing, H. Meng, Y. Guo, L. Yu, R. Li and Q. Peng, *Adv. Mater.*, 2023, **35,** 2208997.

16 C. Guo, Y. Sun, L. Wang, C. Liu, C. Chen, J. Cheng, W. Xia, Z. Gan, J. Zhou, Z. Chen, J. Zhou, D. Liu, J. Guo, W. Li and T. Wang, *Energy Environ. Sci.*, 2024, **17**, 2492–2499.

17 Z. Fu, J. Qiao, F. Cui, W. Zhang, L. Wang, P. Lu, H. Yin, X. Du, W. Qin and X. Hao, *Adv. Mater.*, 2024, **36,** 2313532.

18 D. Qiu, C. Tian, H. Zhang, J. Zhang, Z. Wei and K. Lu, *Adv. Mater.*, 2024, **36,** 2313251.

19 J. Song and Z. Bo, *Chinese Chem. Lett.*, 2023, **34**, 108163.

20 J. Tan, Y. Zhao, G. Li, S. Yang, C. Huang and H. Yu, *Adv. Funct. Mater.*, 2022, **32,** 2209094.

21 Q. Yang, R. Wu, L. Yang, W. Liu, X. Meng, W. Zhang, S. Shen, M. Li, Y. Zhou and J. Song, *Dye. Pigment.*, 2024, **221**, 111808.

22 E. Zhou, J. Cong, Q. Wei, K. Tajima, C. Yang and K. Hashimoto, *Angew. Chemie Int. Ed.*, 2011, **50**, 2799–2803.

23 T. Kim, J.-H. Kim, T. E. Kang, C. Lee, H. Kang, M. Shin, C. Wang, B. Ma, U. Jeong, T.-S. Kim and B. J. Kim, *Nat. Commun.*, 2015, **6**, 8547.

24 H. Yu, M. Pan, R. Sun, I. Agunawela, J. Zhang, Y. Li, Z. Qi, H. Han, X. Zou, W. Zhou, S. Chen, J. Y. L. Lai, S. Luo, Z. Luo, D. Zhao, X. Lu, H. Ade, F. Huang, J. Min and H. Yan, *Angew. Chemie Int. Ed.*, 2021, **60**, 10137–10146.

25 H. Fu, Y. Li, J. Yu, Z. Wu, Q. Fan, F. Lin, H. Y. Woo, F. Gao, Z. Zhu and A. K.-Y. Jen, *J. Am. Chem. Soc.*, 2021, **143**, 2665–2670.

26 T. Liu, T. Yang, R. Ma, L. Zhan, Z. Luo, G. Zhang, Y. Li, K. Gao, Y. Xiao, J. Yu, X. Zou, H. Sun, M. Zhang, T. A. Dela Peña, Z. Xing, H. Liu, X. Li, G. Li, J. Huang, C. Duan, K. S. Wong, X. Lu, X. Guo, F. Gao, H. Chen, F. Huang, Y. Li, Y. Li, Y. Cao, B. Tang and H. Yan, *Joule*, 2021, **5**, 914–930.

27 J. Du, K. Hu, J. Zhang, L. Meng, J. Yue, I. Angunawela, H. Yan, S. Qin, X. Kong, Z. Zhang, B. Guan, H. Ade and Y. Li, *Nat. Commun.*, 2021, **12**, 5264.

28 R. Sun, W. Wang, H. Yu, Z. Chen, X. Xia, H. Shen, J. Guo, M. Shi, Y. Zheng, Y. Wu, W. Yang, T. Wang, Q. Wu, Y. (Michael) Yang, X. Lu, J. Xia, C. J. Brabec, H. Yan, Y. Li and J. Min, *Joule*, 2021, **5**, 1548–1565.

29 Y. Cai, C. Xie, Q. Li, C. Liu, J. Gao, M. H. Jee, J. Qiao, Y. Li, J. Song, X. Hao, H. Y. Woo, Z. Tang, Y. Zhou, C. Zhang, H. Huang and Y. Sun, *Adv. Mater.*, 2023, **35,** 2208165.

30 B. Li, X. Zhang, Z. Wu, J. Yang, B. Liu, Q. Liao, J. Wang, K. Feng, R. Chen, H. Y. Woo, F. Ye, L. Niu, X. Guo and H. Sun, *Sci. China Chem.*, 2022, **65**, 1157–1163.

31 Z. Luo, T. Liu, R. Ma, Y. Xiao, L. Zhan, G. Zhang, H. Sun, F. Ni, G. Chai, J. Wang, C. Zhong, Y. Zou, X. Guo, X. Lu, H. Chen, H. Yan and C. Yang, *Adv. Mater.*, 2020, **32,** 2005942.

32 H. Sun, H. Yu, Y. Shi, J. Yu, Z. Peng, X. Zhang, B. Liu, J. Wang, R. Singh, J. Lee, Y. Li, Z. Wei, Q. Liao, Z. Kan, L. Ye, H. Yan, F. Gao and X. Guo, *Adv. Mater.*, 2020, **32,** 2004183.

33 J. Du, K. Hu, L. Meng, I. Angunawela, J. Zhang, S. Qin, A. Liebman-Pelaez, C. Zhu, Z. Zhang, H. Ade and Y. Li, *Angew. Chemie Int. Ed.*, 2020, **59**, 15181–15185.

34 Y. Wu, S. Schneider, C. Walter, A. H. Chowdhury, B. Bahrami, H.-C. Wu, Q. Qiao, M. F. Toney and Z. Bao, *J. Am. Chem. Soc.*, 2020, **142**, 392–406.

35 H. Yu, Z. Qi, J. Yu, Y. Xiao, R. Sun, Z. Luo, A. M. H. Cheung, J. Zhang, H. Sun, W. Zhou, S. Chen, X. Guo, X. Lu, F. Gao, J. Min and H. Yan, *Adv. Energy Mater.*, 2021, **11,** 2003171.

36 W. Wang, Q. Wu, R. Sun, J. Guo, Y. Wu, M. Shi, W. Yang, H. Li and J. Min, *Joule*, 2020, **4**, 1070–1086.

37 Z. Li, W. Zhong, L. Ying, F. Liu, N. Li, F. Huang and Y. Cao, *Nano Energy*, 2019, **64**, 103931.

38 H. Benten, D. Mori, H. Ohkita and S. Ito, *J. Mater. Chem. A*, 2016, **4**, 5340–5365.

39 X. Liu, C. Zhang, C. Duan, M. Li, Z. Hu, J. Wang, F. Liu, N. Li, C. J. Brabec, R. A. J. Janssen, G. C. Bazan, F. Huang and Y. Cao, *J. Am. Chem. Soc.*, 2018, **140**, 8934–8943.

40 Y. Zhang, B. Wu, Y. He, W. Deng, J. Li, J. Li, N. Qiao, Y. Xing, X. Yuan, N. Li, C. J. Brabec, H. Wu, G. Lu, C. Duan, F. Huang and Y. Cao, *Nano Energy*, 2022, **93**, 106858.

41 N. Wang, X. Long, Z. Ding, J. Feng, B. Lin, W. Ma, C. Dou, J. Liu and L. Wang, *Macromolecules*, 2019, **52**, 2402–2410.

42 G. Wang, F. S. Melkonyan, A. Facchetti and T. J. Marks, *Angew. Chemie Int. Ed.*, 2019, **58**, 4129–4142.

43 L. Zhu, W. Zhong, C. Qiu, B. Lyu, Z. Zhou, M. Zhang, J. Song, J. Xu, J. Wang, J. Ali, W. Feng, Z. Shi, X. Gu, L. Ying, Y. Zhang and F. Liu, *Adv. Mater.*, 2019, **31,** 1902899.

44 B. Liu, H. Sun, J.-W. Lee, J. Yang, J. Wang, Y. Li, B. Li, M. Xu, Q. Liao, W. Zhang, D. Han, L. Niu, H. Meng, B. J. Kim and X. Guo, *Energy Environ. Sci.*, 2021, **14**, 4499–4507.

45 Q. Wu, W. Wang, T. Wang, R. Sun, J. Guo, Y. Wu, X. Jiao, C. J. Brabec, Y. Li and J. Min, *Sci. China Chem.*, 2020, **63**, 1449–1460.

46 M. Xiao, L. Liu, Y. Meng, B. Fan, W. Su, C. Jin, L. Liao, F. Yi, C. Xu, R. Zhang, A. K.-Y. Jen, W. Ma and Q. Fan, *Sci. China Chem.*, 2023, **66**, 1500–1510.

47 Y. Su, Z. Ding, R. Zhang, W. Tang, W. Huang, Z. Wang, K. Zhao, X. Wang, S. Liu and Y. Li, *Sci. China Chem.*, 2023, **66**, 2380–2388.

48 Y. Liu, B. Liu, C.-Q. Ma, F. Huang, G. Feng, H. Chen, J. Hou, L. Yan, Q. Wei, Q. Luo, Q. Bao, W. Ma, W. Liu, W. Li, X. Wan, X. Hu, Y. Han, Y. Li, Y. Zhou, Y. Zou, Y. Chen, Y. Liu, L. Meng, Y. Li, Y. Chen, Z. Tang, Z. Hu, Z.-G. Zhang and Z. Bo, *Sci. China Chem.*, 2022, **65**, 1457–1497.

49 Y. Yao, J. Hou, Z. Xu, G. Li and Y. Yang, *Adv. Funct. Mater.*, 2008, **18**, 1783–1789.

50 F. Zhao, C. Wang and X. Zhan, *Adv. Energy Mater.*, 2018, 2**8,** 1703147.

51 H.-C. Liao, C.-C. Ho, C.-Y. Chang, M.-H. Jao, S. B. Darling and W.-F. Su, *Mater. Today*, 2013, **16**, 326–336.

52 M. A. Brady, G. M. Su and M. L. Chabinyc, *Soft Matter*, 2011, **7**, 11065.

53 S. Bao, H. Yang, H. Fan, J. Zhang, Z. Wei, C. Cui and Y. Li, *Adv. Mater.*, 2021, **33,** 2105301.

54 C. Li, X. Gu, Z. Chen, X. Han, N. Yu, Y. Wei, J. Gao, H. Chen, M. Zhang, A. Wang, J. Zhang, Z. Wei, Q. Peng, Z. Tang, X. Hao, X. Zhang and H. Huang, *J. Am. Chem. Soc.*, 2022, **144**, 14731–14739.

55 K. Hu, C. Zhu, K. Ding, S. Qin, W. Lai, J. Du, J. Zhang, Z. Wei, X. Li, Z. Zhang, L. Meng, H. Ade and Y. Li, *Energy Environ.*

View Article Online
DOI: 10.1039/D4TA06013J

Sci., 2022, **15**, 4157–4166.

56 J. Fu, P. W. K. Fong, H. Liu, C.-S. Huang, X. Lu, S. Lu, M. Abdelsamie, T. Kodalle, C. M. Sutter-Fella, Y. Yang and G. Li, *Nat. Commun.*, 2023, **14**, 1760.

57 C. Fan, H. Yang, Q. Zhang, S. Bao, H. Fan, X. Zhu, C. Cui and Y. Li, *Sci. China Chem.*, 2021, **64**, 2017–2024.

58 J. Song, Y. Li, Y. Cai, R. Zhang, S. Wang, J. Xin, L. Han, D. Wei, W. Ma, F. Gao and Y. Sun, *Matter*, 2022, **5**, 4047–4059.

59 H. Liu, Y. Fu, Z. Chen, J. Wang, J. Fu, Y. Li, G. Cai, C. Su, U. Jeng, H. Zhu, G. Li and X. Lu, *Adv. Funct. Mater.*, 2023, **33,** 2303307.

60 R. Wang, M. Wu, D. Zhang, G. Yang, D. Zheng and J. Yu, *Synth. Met.*, 2024, **304**, 117586.

61 Y.-N. Yang, X.-M. Li, S.-J. Wang, X.-P. Duan, Y.-H. Cai, X.-B. Sun, D.-H. Wei, W. Ma and Y.-M. Sun, *Chinese J. Polym. Sci.*, 2023, **41**, 194–201.

View Article Online
DOI: 10.1039/D4TA06013J

The data supporting this article have been included as part of the Supplementary Information.